SPS hyperon beam Y2 (1989-1994)

High-intensity hyperon beam

In-line with proton beam line to Omega

Ref: Alexandrov et al, NIM A408 (1998) 359-372

Beam Description:

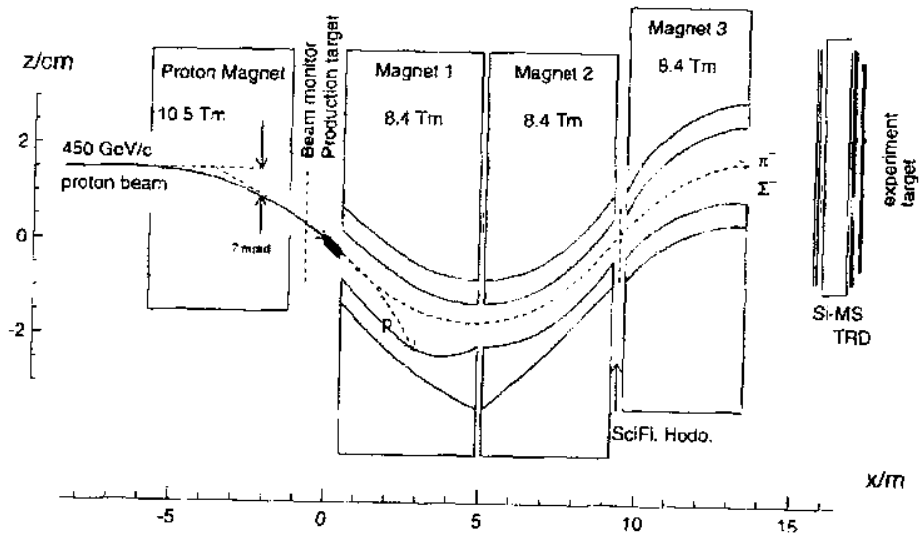

Figure 1: Basic layout of the hyperon beam channel and the target area of experiment WA89

Y2 Beam Composition

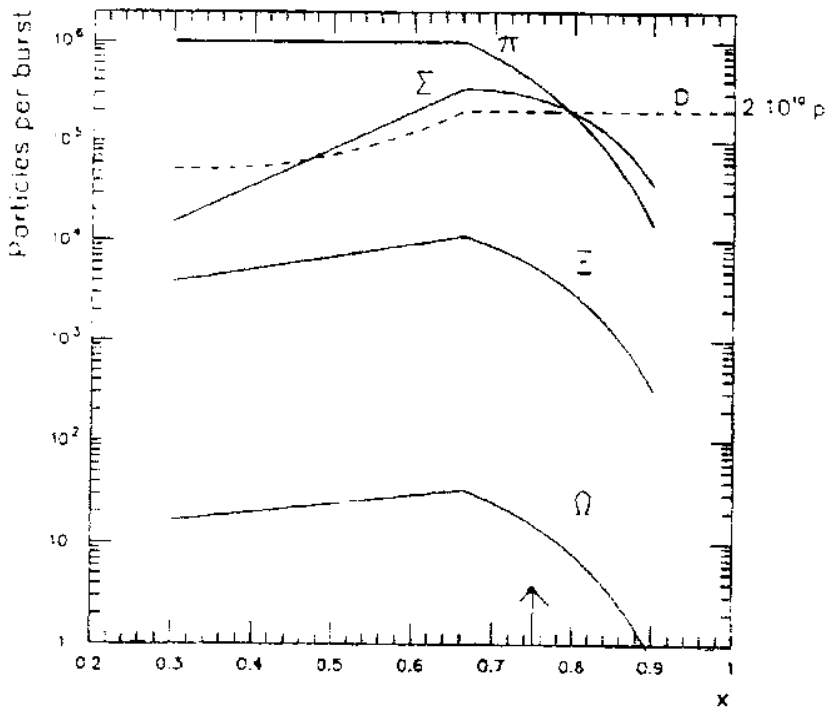

Figure 9: Estimated number of particles per burst reaching the target as a function of x_F. The arrow indicates the working point of WA89.

WA89 experiment (1991)

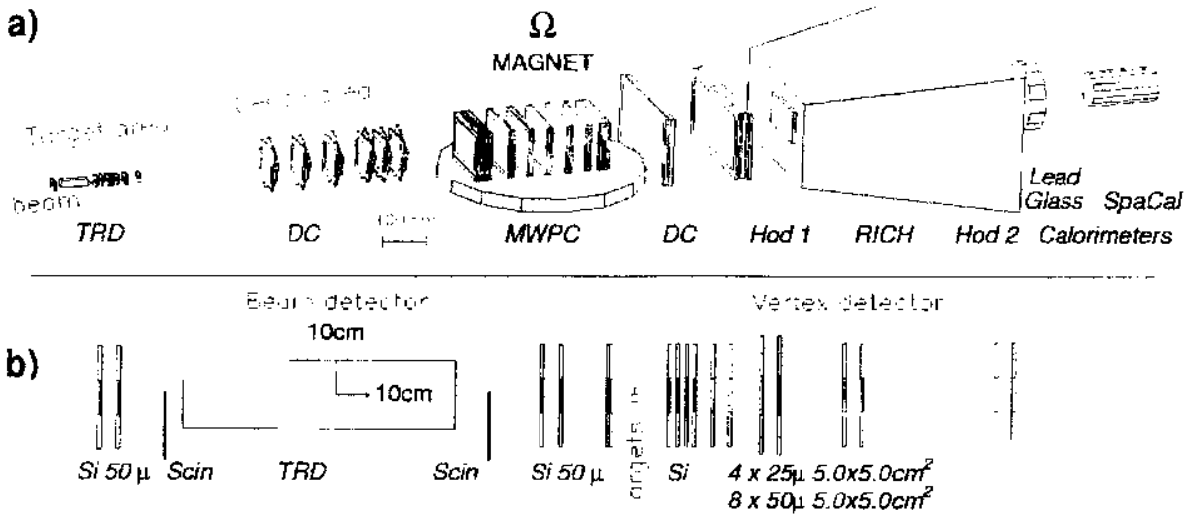

Figure 1: Setup of the WA89 experiment in the 1991 run, a) whole setup, b) the target area

WA89 Beam TRD

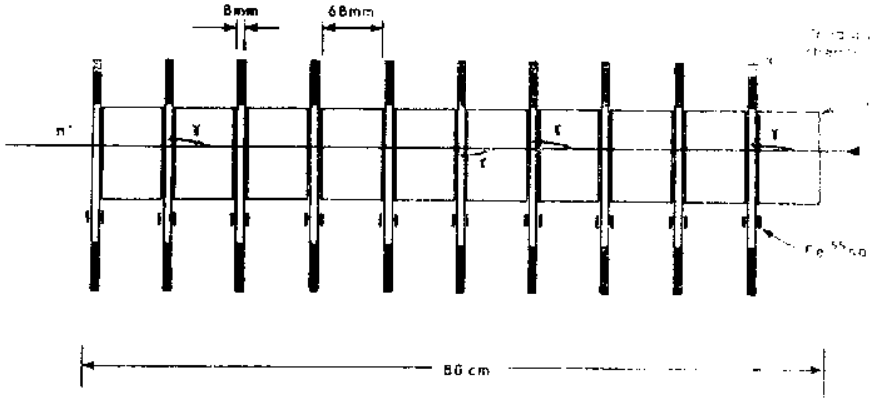

Figure 10: Schematic view of the transition radiation detector. The readout electronics is shown.

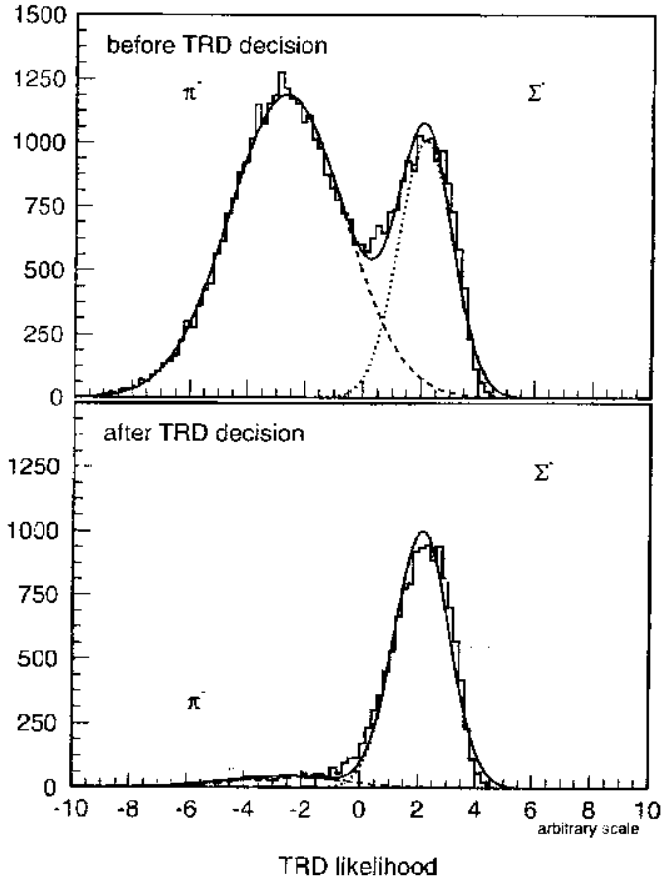

Figure 11: Distributions of TRD likelihoods before and after the TRD decision

10 TRD planes; on-line rejection of π^-;

Σ/π ratio improved from 0.38±0.04 to 10±1

ε=82%; offline Σ^- purity 98.5% with 95%

WA89 (1993/4)

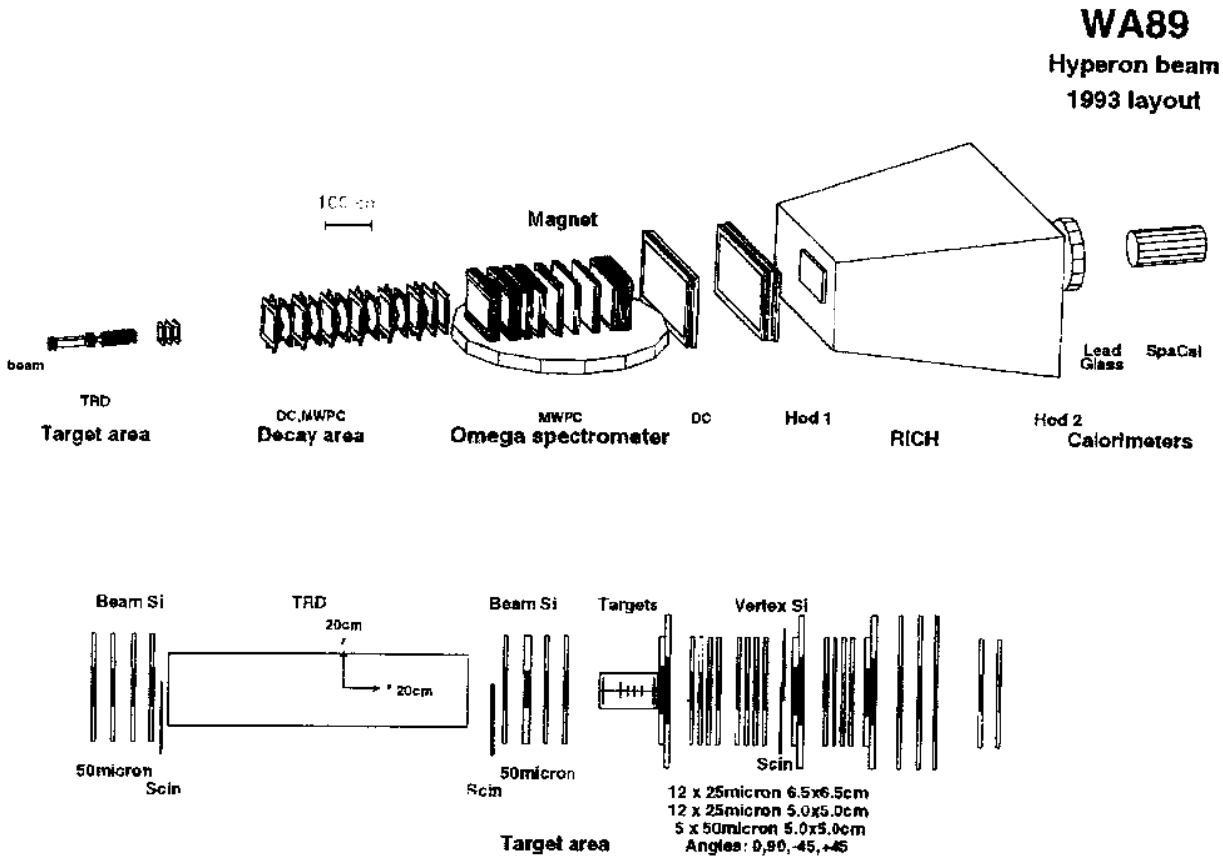

Fig. 1. Setup of the WA89 experiment in the 1993 run. The lower part shows an expanded view of the target area

WA89 features

Hyperon beam ✚ targets ✚ vertex silicon ✚ Λ decay chambers

✚ Omega spectrometer ✚ RICH ✚ EM and hadron calorimeters

- Beam [illegible] Σ^- [illegible] 10^5 π^- per spill (2.5 sec) at 330 GeV [illegible]

  (1993 data → [illegible] × 10^9 Σ^- interactions 1.8 × 10^8 selected [illegible])

- Targets : copper , diamond silicon (approx 5% [illegible] total)
- Silicon : beam 9 planes , vertex - 29 planes 25/50μm [illegible]
- Decay region : [illegible] planes PC (2.5cm) + 32 planes MWPC [illegible]
- Ω : 45 planes MWPC [illegible] field = 1.8 T (7.2 Tm)

  [illegible] = [illegible] GeV/c [illegible] ≈ 10 tracks [illegible]

  mass resolution ≈ [illegible] MeV [illegible]

- RICH : [illegible]

  (p efficiency ≈ 8[illegible] for π rejection ≈ 100 at 100 GeV [illegible])

- Lead glass : $\frac{\sigma(E)}{E} = \frac{7\%}{\sqrt{E}} + 2\%$ $\sigma_x = 0.6$ cm
- Shashl : $\frac{\sigma(E)}{E} = \frac{30\%}{\sqrt{E}} + 2.5\%$ $\sigma_x = \frac{3\text{cm}}{\sqrt{E}} + 0.[illegible]$ cm

  (η^0 mass resolution ≈ [illegible] MeV/c^2)

Data : 6 exabyte drives ≈ 1400 trigger/spill

offline : 800 msec/event 16 x DECstation 5260 (6 months to analyze all of 1993 data)

WA89 event

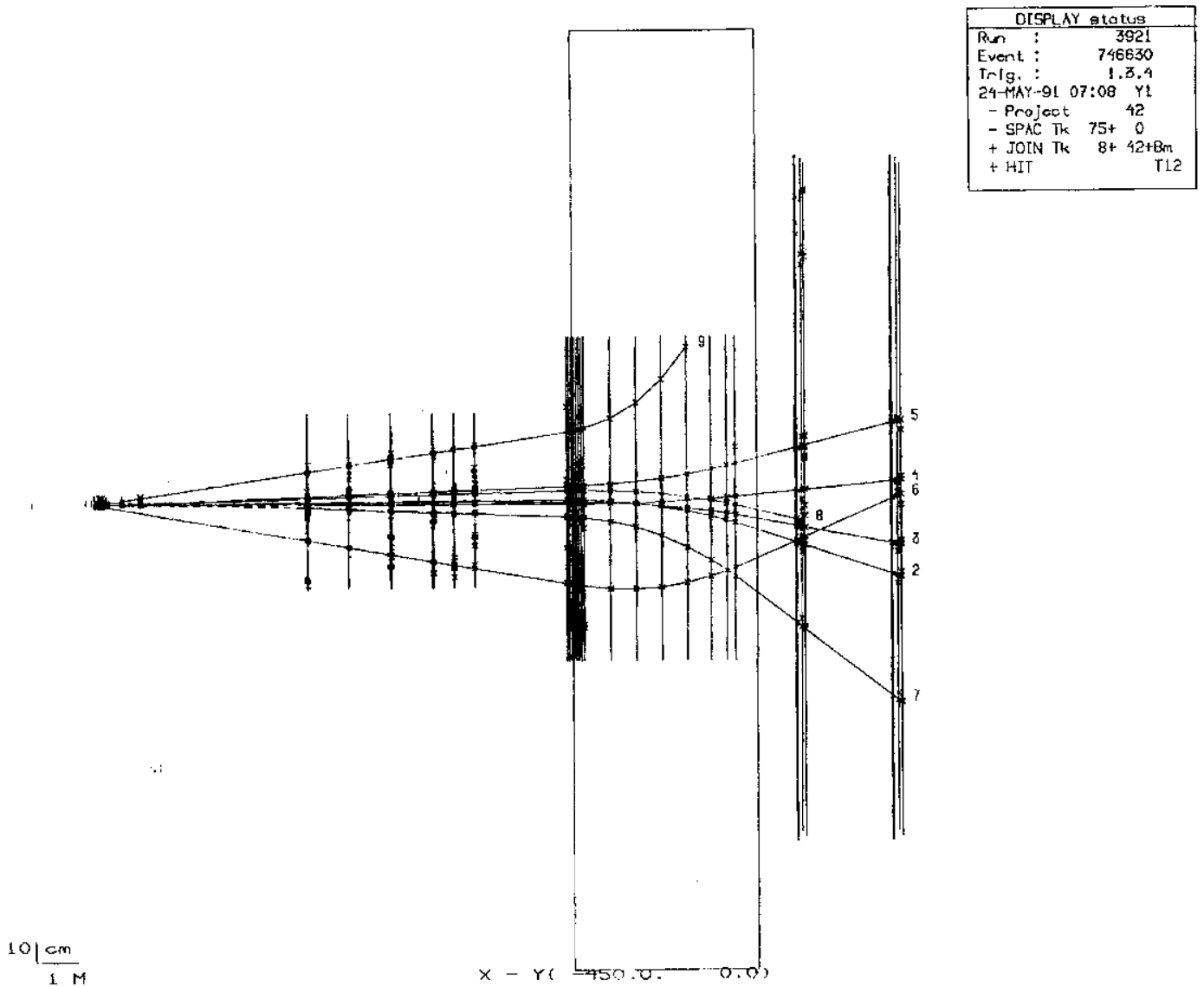
DISPLAY status
Run : 3921
Event : 746630
Trig. : 1.3.4
24-MAY-91 07:08 Yt
- Project 42
- SPAC Tk 75+ 0
+ JOIN Tk 8+ 42+Bm
+ HIT T12
9
5
6
8
3
2
7
10 cm
1 M
X - Y(-450.0. 0.0)

Walk-in RICH

Ref: NIM A 371, 27 (1996)

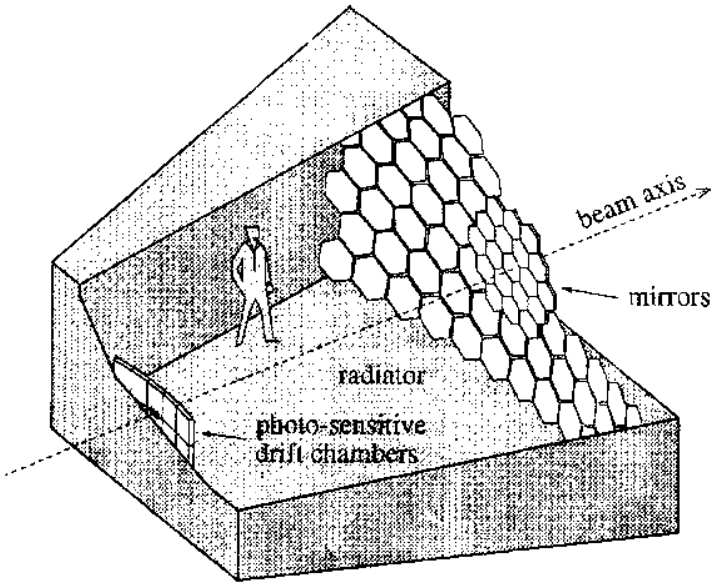

Figure 2: Overall view of the Omega RICH in WA89.

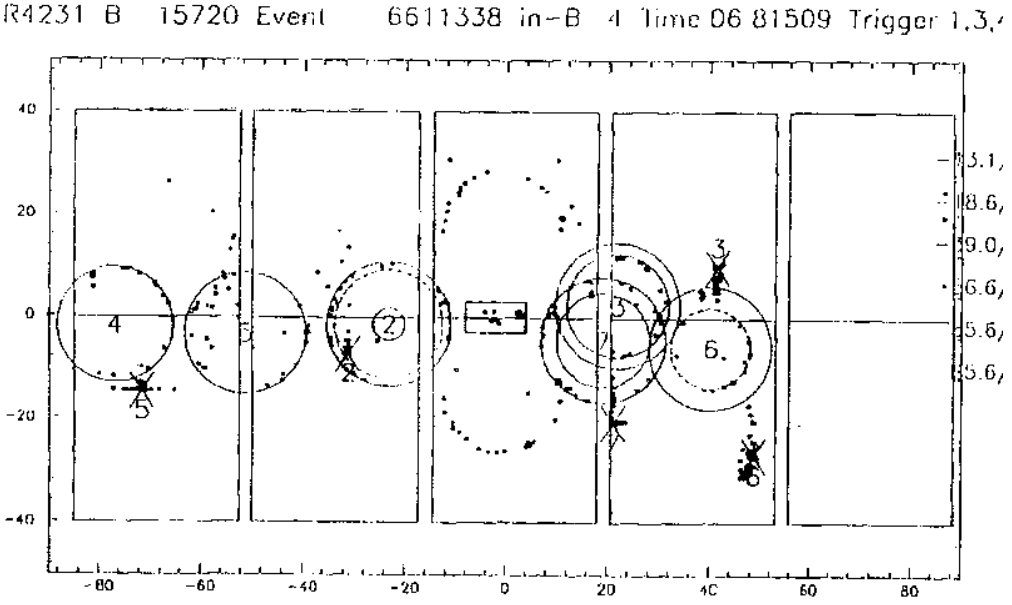

WA89 Ξ^- production by Σ^-, n, π^-

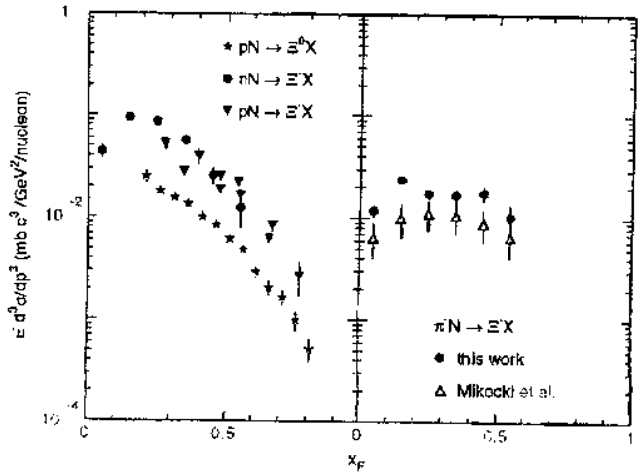

Fig. 7. Left part: Invariant cross sections for inclusive Ξ^- and Ξ^0 production at $p_t^2 < 0.2$ GeV$^2/c^2$ by protons and neutrons: $nA \to \Xi^- X$ at 345 GeV/c this measurement (*filled circles*); $pA \to \Xi^- X$ at 200 GeV/c and 400 GeV/c [22, 26] (*triangles*); $pA \to \Xi^0 X$ at 400 GeV/c [27] (*stars*). The right part compares the invariant inclusive Ξ^- production cross sections at $p_t^2 < 0.2$ GeV$^2/c^2$ by pions observed in the present experiment at 345 GeV/c (*filled circles*), to previous data taken at 200 GeV/c (*open triangles*) [34]. Only statistical errors are given. For the discussion on systematic uncertainties refer to the text

Z.Phys.C 76, 35 (1997)

WA89 $\Xi^*(1690) \rightarrow \Xi^-\pi^+$

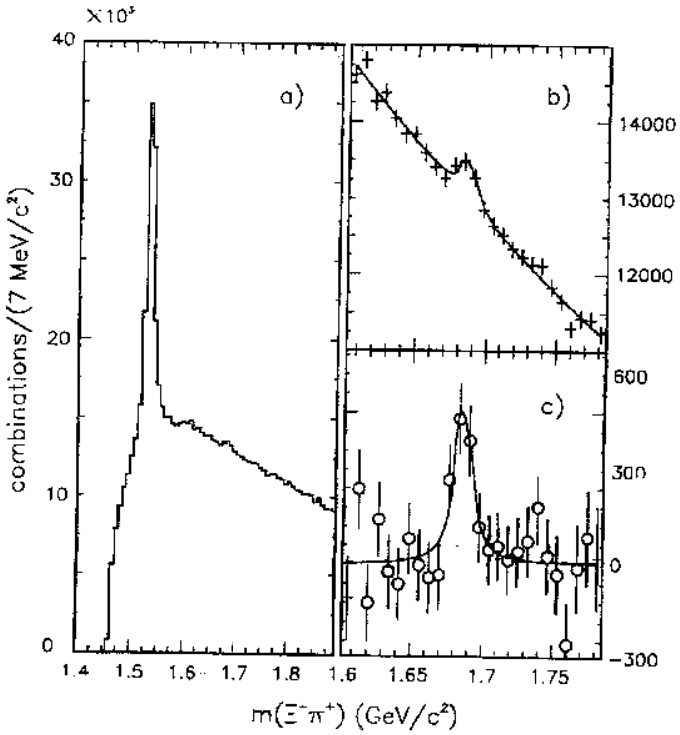

Figure 1: **Invariant mass distribution of the $\Xi^-\pi^+$ combinations. a) the $\Xi^0(1530)$ and $\Xi^0(1690)$ mass region; b) the $\Xi^0(1690)$ mass region only; c) the $\Xi^0(1690)$ mass region after background subtraction.**

Eur.Phys.J.C5, 621 (1998)

WA89 silicon tracking

Target region:

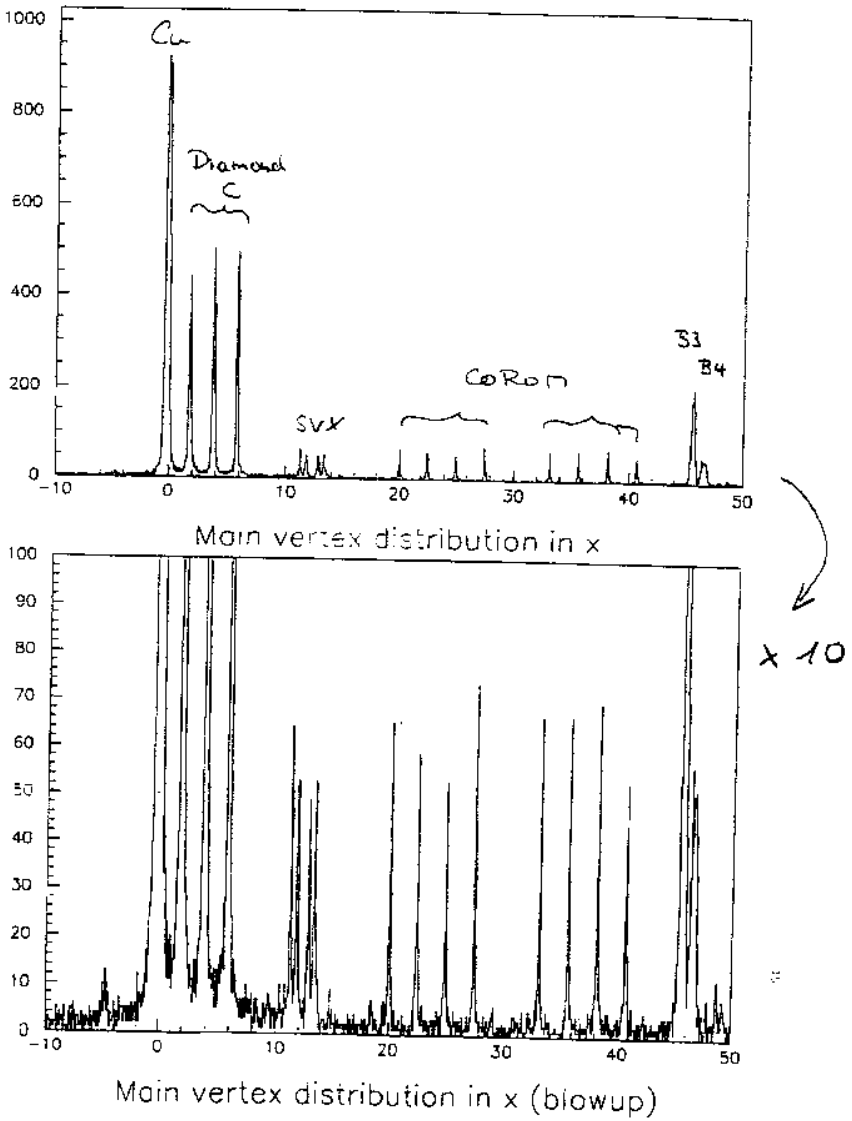

WA89 charm with RICH

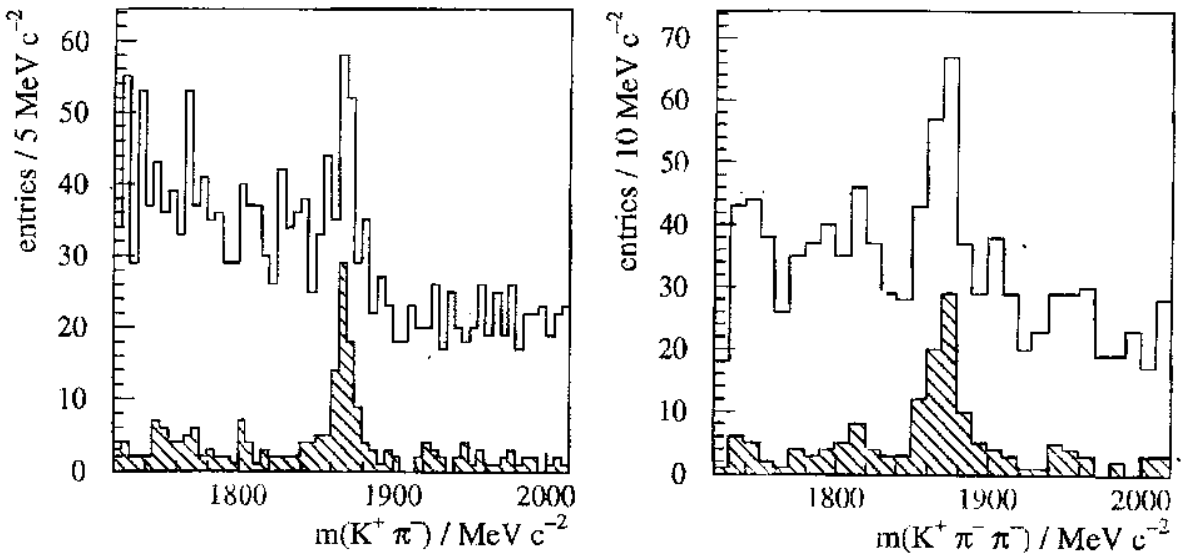

Figure 9: Invariant mass plots for $\overline{D^0} \to K^+\pi^-$ (left) and $D^- \to K^+\pi^-\pi^-$ (right), with weak (solid line) and strong (hatched area) RICH identification.

WA89 Charm Asymmetries

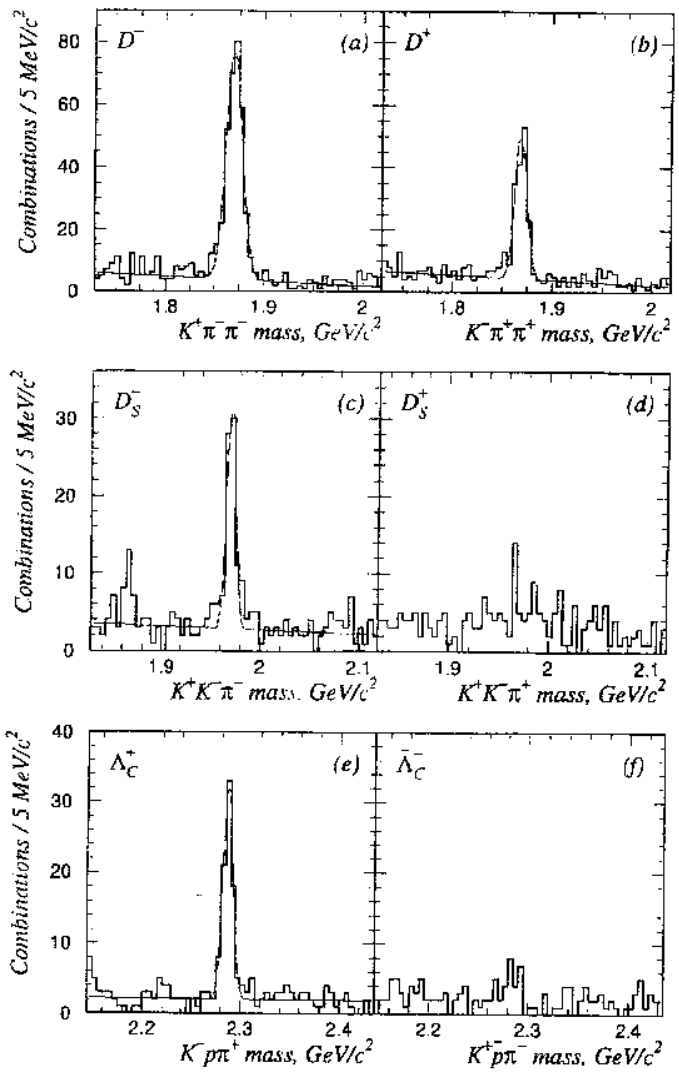

Figure 2: Invariant mass distributions for (a) $D^- \to K^+\pi^-\pi^-$, (b) $D^+ \to K^-\pi^+\pi^+$, (c) $D_s^- \to K^+K^-\pi^-$, (d) $D_s^+ \to K^-K^+\pi^+$, (e) $\Lambda_c \to K^-p\pi^+$, (f) $\overline{\Lambda}_c \to K^+\overline{p}\pi^-$.

WA89 $D^{\pm}$ efficiency

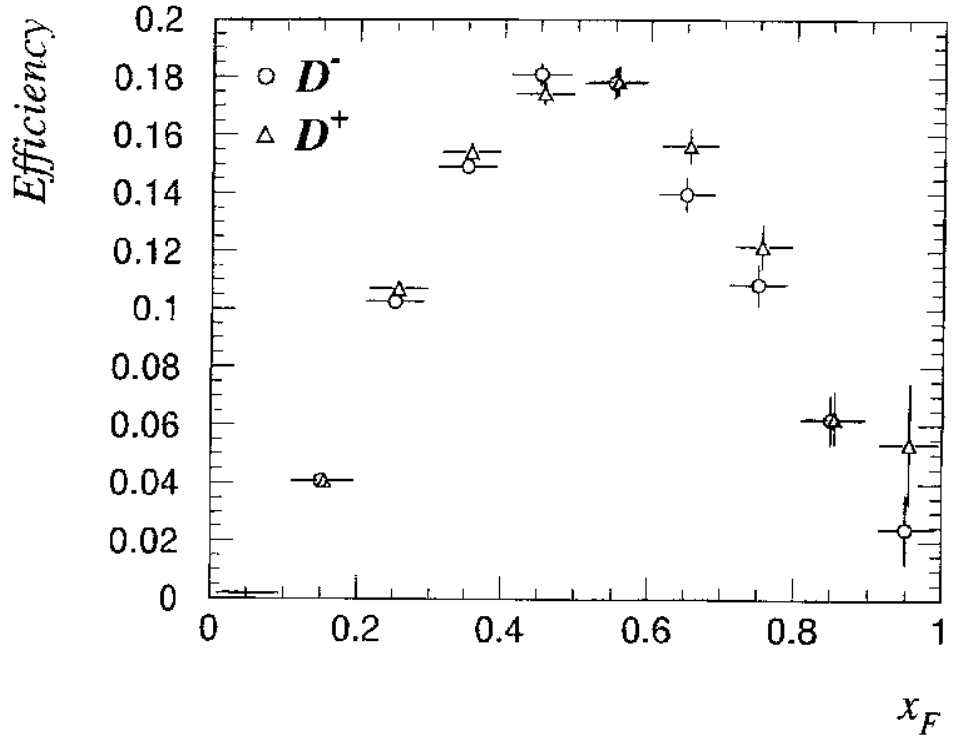

Figure 3: Full efficiency of $D^{\pm}$ meson reconstruction. The average values for the 1993 and 1994 runs of data taking are shown.

WA89 charm asymmetries

Eur.Phys.J
C8, 593 (1999)

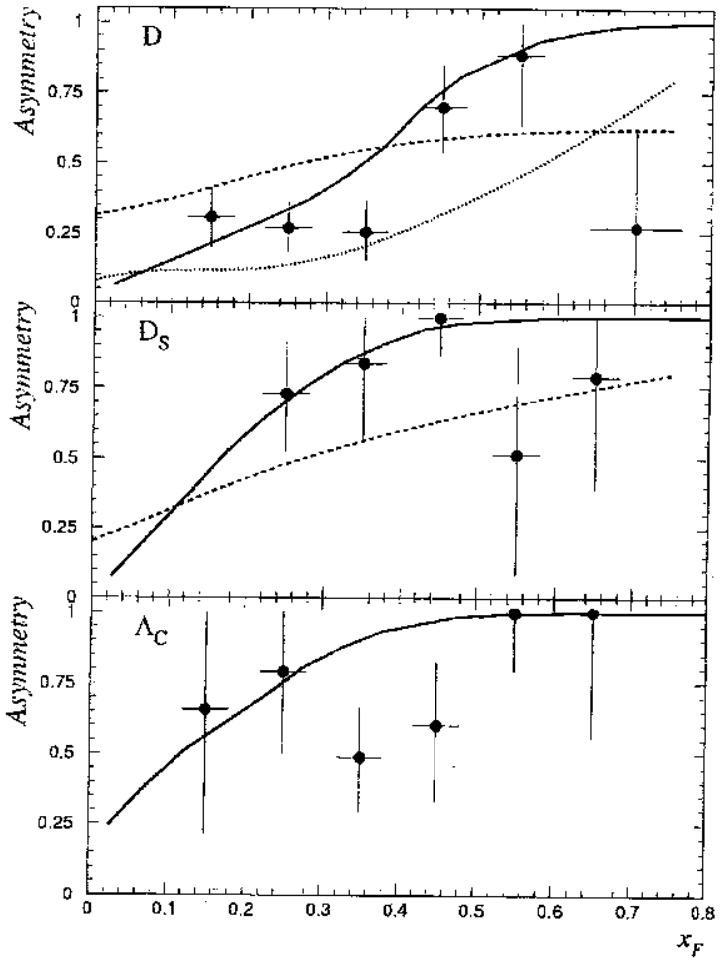

Figure 4: Asymmetries for $D^{\pm}$, D_s, and Λ_c production. The solid and dashed curves show the results of calculations [26] and [28], respectively. The dotted curve shows the tuned PYTHIA calculations for π^- beam taken from [6], which represent closely the results obtained by experiment E791 at FNAL.

Total c/cbar production by Σ^-

Submitted to Eur.Phys.J.

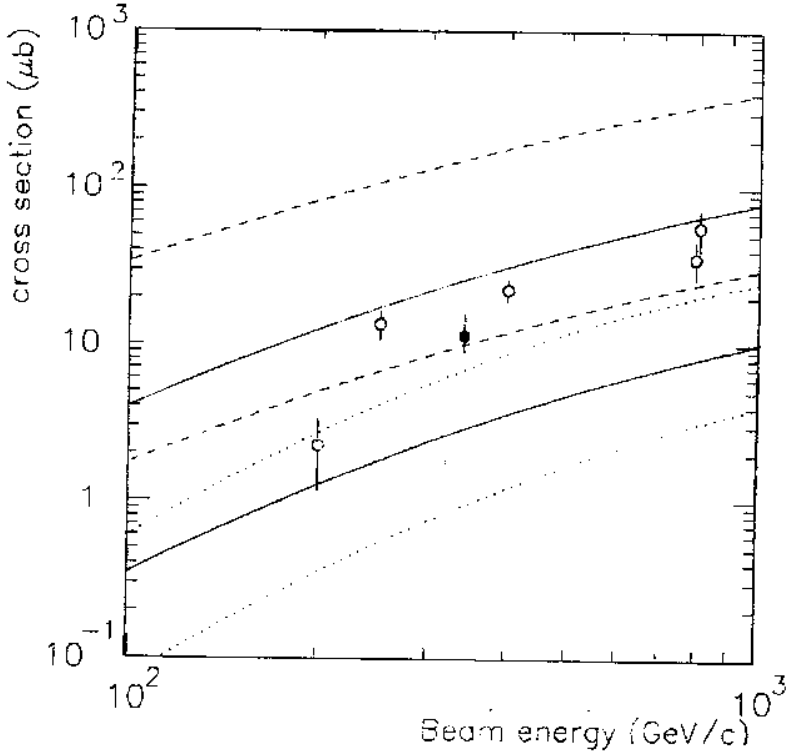

Figure 5: Total charm production cross sections by Σ^- (this expt., full circle) and protons (open circles) compared to theoretical predictions (bands for different charm-quark masses as explained in the text).

WA89: Σ^- - e^- elastic scattering

Mean square charge radius, $\langle r^2_{ch} \rangle (\Sigma^-)$

$= 0.91 \pm 0.32_{stat} \pm 0.4_{syst}$ fm^2

Eur.Phys.J C8, 59 (1999)

WA89: Production of Ξ^* resonances in Σ^- induced reactions at 345 GeV/c

Submitted to Eur.Phys.J.

Coming soon: Polarization of hyperons produced by 345 GeV/c Σ^-